Low Complexity Estimation of Frequency Selective Channels for the LTE-A Uplink

Stefan Pratschner, Erich Zöchmann, *Student Member, IEEE*, and Markus Rupp, *Fellow, IEEE*

***Abstract*—3GPP LTE-A uplink channel estimation is based on pilot symbols. For the support of MIMO transmissions, a special reference symbol structure was standardized to perform MIMO channel estimation without excessive overhead. We propose a low complexity channel estimation method in the frequency domain based on correlation that exploits the orthogonal structure of the reference symbols to mitigate inter-layer interference. Further, we introduce a smoothing method to deal with the interference that leads to improved performance at low signal to noise ratio.**

***Index Terms*—LTE-A, uplink, channel estimation, DMRS.**

I. Introduction

SINCE Release 10 3GPP LTE-A supports MIMO transmissions in the uplink. This requires modified or new methods for channel estimation (CE) in order to perform coherent detection. Many authors investigated discrete Fourier transform (DFT) or discrete cosine transform (DCT) based CE methods and considered separating the channel impulse responses (CIR) in time domain [1]–[5]. These methods suffer from CIR overlaps in time domain, which is referred to as CIR energy leakage. On the other hand, estimating the channel in frequency domain leads to inter-layer interference due to the allocation of reference symbols on the same time and frequency resources for every spatial layer. Therefore, the reference symbols are designed to be orthogonal in code domain but in general a frequency selective channel destroys this orthogonality [6], [7].

For physically meaningful channels, neighbouring subcarriers will be correlated within the coherence bandwidth [8]. We utilize this property to perform frequency domain CE of frequency selective channels on the LTE-A physical uplink shared channel (PUSCH). Since we do not consider time domain CE, our methods do not suffer from CIR leakage. First we present a minimum mean square error (MMSE) estimator that will serve as a performance reference. Then we introduce a low complexity frequency domain CE method based on correlation (matched filtering) with the reference symbols. We analyse the reference symbol structure and mitigate the occurring inter-layer interference exploiting its orthogonal structure. Another method exploiting channel correlations is quadratic smoothing (QS). This scheme cannot remove the inter-layer interference entirely, which manifests in a higher error floor, but shows improved performance at lower SNR in return.

Manuscript received April 23, 2015; accepted September 21, 2015. Date of publication September 23, 2015; date of current version December 15, 2015. This work was supported by A1 Telekom Austria AG and the Institute of Telecommunications, TU Wien. The associate editor coordinating the review of this paper and approving it for publication was B. Shim.

The authors are with the Institute of Telecommunications, TU Wien, 1040 Wien, Austria (e-mail: spratsch@nt.tuwien.ac.at; ezoechma@nt.tuwien.ac.at; mrupp@nt.tuwien.ac.at).

Color versions of one or more of the figures in this paper are available online at http://ieeexplore.ieee.org.

Digital Object Identifier 10.1109/LWC.2015.2481428

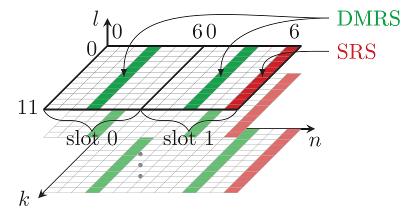

Fig. 1. The LTE-A uplink reference symbol allocation in two slots (one subframe).

II. System Model

As introduced in [9], [10], the LTE-A uplink employs single carrier frequency division multiplexing (SC-FDM), which is essentially DFT spreaded orthogonal frequency division multiplexing (OFDM). We follow the notation introduced in [10] and denote vectors and matrices by bold symbols. Our MIMO-OFDM system with subcarrier index $k \in \{0, \cdots, B-1\}$ is denoted by vectors of size B. The pilot symbols $\boldsymbol{r}^{(l)} \in \mathbb{C}^B$ of layer l are added after DFT spreading, right before precoding. As the channel estimation takes place right after the receiver's DFT, the system model for CE amounts to an OFDM system. We assume a sufficient cyclic prefix (CP) length, so that the frequency domain channel matrices $\boldsymbol{H}^{(i,l)} \in \mathbb{C}^{B\times B}$ of the effective channel (including the precoder) from layer $l \in \{1, \ldots, L\}$ to receive antenna $i \in \{1, \ldots, N_R\}$ are diagonal. For channel estimation we only exploit the system model at time $n = 3$ in each slot where the demodulation reference signals (DMRS) are multiplexed in the time frequency resource grid as shown in Fig. 1. We therefore omit the time index n in the following. The received signal on antenna i is

$$\boldsymbol{y}^{(i)} = \sum_{l=1}^{L} \boldsymbol{H}^{(i,l)}\boldsymbol{r}^{(l)} + \boldsymbol{z}^{(i)} = \sum_{l=1}^{L} \boldsymbol{R}^{(l)}\boldsymbol{h}^{(i,l)} + \boldsymbol{z}^{(i)}, \quad (1)$$

with the additive zero mean, i.i.d. Gaussian noise $\boldsymbol{z}^{(i)} \sim \mathcal{CN}\{0, \sigma_z^2\boldsymbol{I}\}$. Here $\boldsymbol{h}^{(i,l)}$ consists of the elements of the diagonal matrix $\boldsymbol{H}^{(i,l)}$ and $\boldsymbol{R}^{(l)} = \mathrm{diag}(\boldsymbol{r}^{(l)})$, where the diag operator constructs a diagonal matrix. Since we estimate the channel only once per slot, interpolation in time has to be carried out to obtain channel estimates for the whole resource grid. Finding the optimal interpolation function is out of the scope of this work. Assuming the channel coherence time to be larger than the slot duration (block fading) we assign the obtained channel estimate to all OFDM symbols in one slot.

III. Reference Symbols

In a PUSCH transmission of the LTE-A uplink, a DMRS occupies the whole scheduled user bandwidth B (in numbers of subcarriers). The reference symbols are defined in [11] and are explained in more detail in [1], [5].

We assume that the user is assigned B subcarriers starting at 0, i.e., $k \in \{0, 1, \ldots, B-1\}$. We denote the base sequence on the B scheduled subcarriers for one slot by $\boldsymbol{b} \in \mathbb{C}^B$ where we do not consider any group or sequence hopping [11] because it it not relevant for our proposed methods. The base sequences $\boldsymbol{b}$ are complex exponential sequences lying on the unit circle fulfilling

$$\text{diag}(\boldsymbol{b})^H \text{diag}(\boldsymbol{b}) = \boldsymbol{I}_B, \tag{2}$$

where $(\cdot)^H$ denotes the Hermitian transpose. In LTE-A the DMRS of different transmission layers in the same slot are orthogonal in terms of frequency domain code division multiplexing (FD-CDM) [1]. This is obtained by cyclically shifting the base sequence. Similar to [12], DMRS on layer l for one slot are given by

$$\boldsymbol{R}^{(l)} = \boldsymbol{T}^{(l)} \text{diag}(\boldsymbol{b}), \tag{3}$$

with the cyclic shift operator

$$\boldsymbol{T}^{(l)} = \text{diag}\left(e^{j0}, \ldots, e^{j\alpha_l k}, \ldots, e^{j\alpha_l (B-1)}\right), \tag{4}$$

and the layer dependent cyclic shift α_l. We further conclude from (2)–(4) that $\left(\boldsymbol{R}^{(l)}\right)^H = \left(\boldsymbol{R}^{(l)}\right)^{-1}$ which implies $\left(\boldsymbol{R}^{(l)}\right)^H \boldsymbol{R}^{(l)} = \boldsymbol{I}_B$. As we will see in Section IV, the inter-layer interference is determined by the correlation of two reference symbols. Using (2) the product of two DMRS from layers l and u with $l, u \in \{1, \ldots, L\}$, becomes

$$\begin{aligned}\left(\boldsymbol{R}^{(l)}\right)^H \boldsymbol{R}^{(u)} &= \text{diag}(\boldsymbol{b})^H \left(\boldsymbol{T}^{(l)}\right)^H \boldsymbol{T}^{(u)} \text{diag}(\boldsymbol{b}) \\ &= \text{diag}\left(e^{j0} \ \ldots \ e^{j\Delta\alpha_{u,l} k} \ \ldots \ e^{j\Delta\alpha_{u,l}(B-1)}\right),\end{aligned} \tag{5}$$

with $\Delta\alpha_{u,l} = \alpha_u - \alpha_l$. Due to the FD-CDM orthogonality, summing the elements of (5) evaluates to zero for different layers, i.e., $\text{trace}((\boldsymbol{R}^{(l)})^H \boldsymbol{R}^{(u)}) = 0$ for $u \neq l$. However, this orthogonality is in general destroyed by a frequency selective channel.

IV. Channel Estimation

A. Minimum Mean Square Error Estimation

In this section we introduce an MMSE estimator that leads to the best performance in terms of MSE and will provide a lower bound on the CE MSE. This performance however, comes at the cost of high complexity and therefore, all our proposed methods will lead to an inferior MSE performance but have lower complexity than MMSE estimation.

System model (1) can be compactly written as

$$\boldsymbol{y}^{(i)} = \underline{\boldsymbol{R}}\underline{\boldsymbol{h}}^{(i)} + \boldsymbol{z}^{(i)}, \tag{6}$$

where $\underline{\boldsymbol{R}} = (\boldsymbol{R}^{(1)} \ldots \boldsymbol{R}^{(L)})$ and $\underline{\boldsymbol{h}}^{(i)} = \left((\boldsymbol{h}^{(i,1)})^T \ldots (\boldsymbol{h}^{(i,L)})^T\right)^T$. The MMSE CE for receive antenna i is given by

$$\hat{\underline{\boldsymbol{h}}}^{(i)}_{\text{MMSE}} = \arg\min_{\hat{\underline{\boldsymbol{h}}}^{(i)}} \mathbb{E}\left\{\left\|\hat{\underline{\boldsymbol{h}}}^{(i)} - \underline{\boldsymbol{h}}^{(i)}\right\|_2^2\right\}, \tag{7}$$

which leads to the known solution [13]

$$\hat{\underline{\boldsymbol{h}}}^{(i)}_{\text{MMSE}} = \left(\sigma^2_{z^{(i)}}\left(\boldsymbol{C}_{\underline{\boldsymbol{h}}^{(i)}} + \varepsilon \boldsymbol{I}_{LB}\right)^{-1} + \underline{\boldsymbol{R}}^H \underline{\boldsymbol{R}}\right)^{-1} \underline{\boldsymbol{R}}^H \boldsymbol{y}^{(i)}, \tag{8}$$

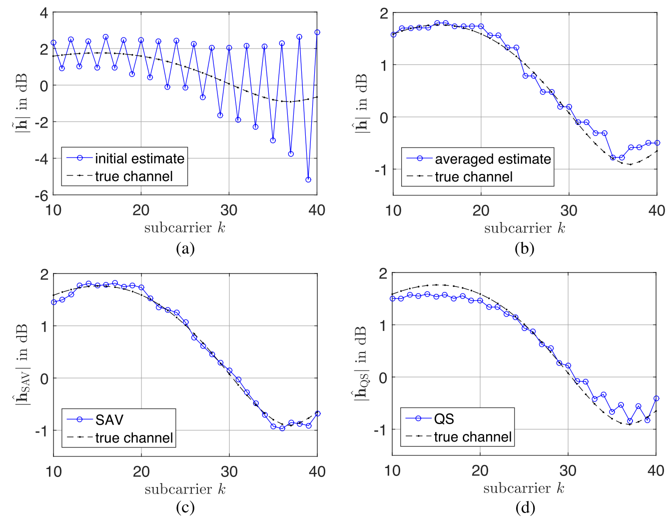

Fig. 2. Exemplary channel estimates for a TU channel realization in a 2 × 2 system with $L = \gamma = 2$ at 25 dB SNR. (a) Initial estimate. (b) Averaged estimate for $\bar{\gamma} = 2$. (c) Sliding averaged estimate. (d) Quadratically smoothed estimate.

with $\boldsymbol{C}_{\underline{\boldsymbol{h}}^{(i)}} = \mathbb{E}\{\underline{\boldsymbol{h}}^{(i)} \underline{\boldsymbol{h}}^{(i)H}\}$, which is augmented by the regularisation term $\varepsilon \boldsymbol{I}_{LB}$, with $\varepsilon \geq 0$, for numerical stability.

B. Correlation Based Estimation

To obtain a channel estimate for the channel $\boldsymbol{h}^{(i,l)}$ from layer l to receive antenna i we correlate the received signal with the reference symbol of layer l

$$\tilde{\boldsymbol{h}}^{(i,l)} = \left(\boldsymbol{R}^{(l)}\right)^H \boldsymbol{y}^{(i)}. \tag{9}$$

Inserting our system model (1), we obtain

$$\begin{aligned}\tilde{\boldsymbol{h}}^{(i,l)} &= \left(\boldsymbol{R}^{(l)}\right)^H \sum_{u=1}^{L} \boldsymbol{R}^{(u)} \boldsymbol{h}^{(i,u)} + \left(\boldsymbol{R}^{(l)}\right)^H \boldsymbol{z}^{(i)} \\ &= \boldsymbol{h}^{(i,l)} + \underbrace{\sum_{\substack{u=1 \\ u \neq l}}^{L} \left(\boldsymbol{R}^{(l)}\right)^H \boldsymbol{R}^{(u)} \boldsymbol{h}^{(i,u)}}_{\text{inter-layer interference}} + \tilde{\boldsymbol{z}}^{(i)}.\end{aligned} \tag{10}$$

Here $\tilde{\boldsymbol{z}}^{(i)}$ has the same distribution as $\boldsymbol{z}^{(i)}$ since $\left(\boldsymbol{R}^{(l)}\right)^H$ is unitary and introduces phase changes only. Due to the allocation of DMRS on the same time and frequency resources on different spatial layers, the initial estimate of one MIMO channel suffers from interference of other layers. The inter-layer interference in (10) is severe as illustrated in Fig. 2(a) making the initial estimate unsuited for coherent detection.

V. Interference Cancellation

We conclude from (5) that the interference in (10) is characterized by a rotation on the unit circle in the complex plane as illustrated in Fig. 3. The phase shift between two adjacent points in frequency is determined by $\Delta\alpha_{u,l}$ and the number of distinct points on the unit circle is given by $\gamma = 2\pi/\Delta\alpha_{u,l}$. The key observation is that summing (5) over a complete turn on the unit circle will cancel the interference. For this

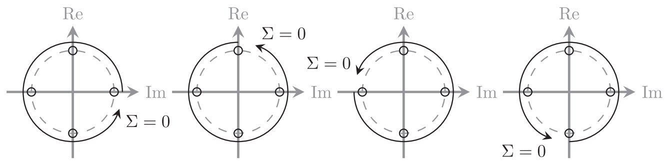

Fig. 3. The inter-layer interference on the unit circle is cancelled when summed over all points.

TABLE I
PHASE SHIFT FOR POSSIBLE NUMBERS OF LAYERS L

L	1	2	3	4
$\Delta\alpha_{u,l}$	$\{0\}$	$\{0, \pm\pi\}$	$\{0, \pm\pi/2, \pm\pi\}$	$\{0, \pm\pi/2, \pm\pi\}$
$\bar{\gamma}$	1	2	4	4

we have to sum, or average, over γ consecutive elements of $\tilde{\boldsymbol{h}}^{(i,l)}$.

The phase shift $\Delta\alpha_{u,l} = \alpha_u - \alpha_l$ and therefore the periodicity γ of the interference is dependent on the two layers u and l. When estimating all MIMO channels exploiting (10) all possible combinations of $u, l \in \{1, \ldots, L\}$ appear and therefore different values of $\Delta\alpha_{u,l}$ will occur in the inter-layer interference term. Studying [11], one can relate the possible occurring phase shifts to the number of active spatial layers as listed in Table I. In order to cancel all interference terms at once we have to sum over the largest possible number of points on the unit circle, i.e., the largest possibly occurring periodicity which we denote by $\bar{\gamma}$. The corresponding values of $\bar{\gamma}$ are listed in Table I, where $L \leq 4$ in the LTE-A uplink.

From this we conclude that the sum of $\bar{\gamma}$ consecutive elements in (5) will evaluate to zero, independent on the actual layers u and l. As a consequence for CE, when we sum (average) the initial estimate (10) over $\bar{\gamma}$ adjacent subcarriers k, all products of different ($u \neq l$) DMRS will vanish and the FD-CDM orthogonality will be preserved [7]. We exploit this property in our low complexity correlation based channel estimation method in Section V-A.

A. Averaging

The special structure of the reference symbols allows us to mitigate the inter-layer interference in the initial estimate. As previously explained, summing the initial estimate $\tilde{\boldsymbol{h}}^{(i,l)}$ over $\bar{\gamma}$ adjacent subcarriers cancels the inter-layer interference. This leads to the idea of piecewise averaging the initially obtained estimate over $\bar{\gamma}$ adjacent elements. This in turn means that we have to assume the channel to be frequency flat on $\bar{\gamma}$ consecutive subcarriers. This would result in a piecewise averaged channel estimate that is constant on $\bar{\gamma}$ consecutive subcarriers as shown in Fig. 2(b).

It suffices to sum over all points of interference on the unit circle while it actually does not matter where the summation starts and stops as illustrated in Fig. 3. Therefore we can augment this method to a sliding average. Here, the averaging window of size $\bar{\gamma}$ is shifted subcarrier by subcarrier over the scheduled bandwidth. The sliding average is given by

$$\hat{\boldsymbol{h}}_{\text{SAV}}^{(i,l)}[k] = \frac{1}{\bar{\gamma}^2} \sum_{t=k-\bar{\gamma}+1}^{k} \sum_{j=t}^{t+\bar{\gamma}-1} \tilde{\boldsymbol{h}}^{(i,l)}[j], \tag{11}$$

for $\bar{\gamma} \leq k \leq B - \bar{\gamma} + 1$ where square brackets denote elements of a vector. The second sum describes the averaging of $\bar{\gamma}$ elements while the first sum describes the shift of this averaging window. Using this augmentation the channel estimate is not piecewise constant any more and changes from subcarrier to subcarrier as shown in Fig. 2(c). Still this method exploits the DMRS structure and cancels the inter-layer interference.

B. Quadratic Smoothing

The initial correlator estimate solves the decoupled least squares estimation problem for the channel $\boldsymbol{h}^{(i,l)}$ from layer l to receive antenna i, ignoring the other channels

$$\tilde{\boldsymbol{h}}^{(i,l)} = \underset{\boldsymbol{h}^{(i,l)}}{\arg\min} \left\| \boldsymbol{y}^{(i)} - \boldsymbol{R}^{(l)} \boldsymbol{h}^{(i,l)} \right\|_2^2. \tag{12}$$

The unitary structure of the DMRS yields

$$\tilde{\boldsymbol{h}}^{(i,l)} = \left(\left(\boldsymbol{R}^{(l)}\right)^H \boldsymbol{R}^{(l)} \right)^{-1} \left(\boldsymbol{R}^{(l)}\right)^H \boldsymbol{y}^{(i)} = \left(\boldsymbol{R}^{(l)}\right)^H \boldsymbol{y}^{(i)},$$

which is identical to (9). This observation together with the previous assumption of correlated subcarriers leads to the idea of augmenting (12) by a frequency smoothness constraint. Quadratic smoothing [14] with a matrix $\boldsymbol{Q} \in \mathbb{R}^{(B-1)\times B}$

$$\boldsymbol{Q} = \begin{pmatrix} -1 & 1 & & & \\ & -1 & 1 & & \\ & & \ddots & \ddots & \\ & & & -1 & 1 \end{pmatrix} \tag{13}$$

can be formulated as a convex minimization problem

$$\hat{\boldsymbol{h}}_{\text{QS}}^{(i,l)} = \underset{\boldsymbol{h}^{(i,l)}}{\arg\min} \left\| \boldsymbol{y}^{(i)} - \boldsymbol{R}^{(l)} \boldsymbol{h}^{(i,l)} \right\|_2^2 + \lambda \left\| \boldsymbol{Q} \boldsymbol{h}^{(i,l)} \right\|_2^2, \tag{14}$$

with the known result

$$\hat{\boldsymbol{h}}_{\text{QS}}^{(i,l)} = \left(\boldsymbol{I}_B + \lambda \boldsymbol{Q}^H \boldsymbol{Q}\right)^{-1} \underbrace{\left(\boldsymbol{R}^{(l)}\right)^H \boldsymbol{y}^{(i)}}_{\tilde{\boldsymbol{h}}^{(i,l)}}. \tag{15}$$

Similar to (11) this can be interpreted as another way to cope with the inter-layer interference in (10) by post processing. This method does not use the DMRS structure explicitly but suppresses the interference by smoothing. It is therefore not able to cancel the complete inter-layer interference as depicted in Fig. 2(d).

The value of λ can be interpreted as the prior about the channel [15] as it reflects its frequency selectivity. The choice of λ poses another optimization problem where the optimal value depends on the number of used layers L. The minimum w.r.t. λ is rather broad and minima obtained for different channel models lie close to each other. This allows λ to be fixed for practical realisations such that the matrix inverse in (15) can be precomputed, in our simulations λ was fixed to $\lambda = 8$.

VI. SIMULATIONS AND COMPLEXITY

All our simulations were carried out by the Vienna LTE-A uplink simulator [16], [17]. We assume a single user 2×2

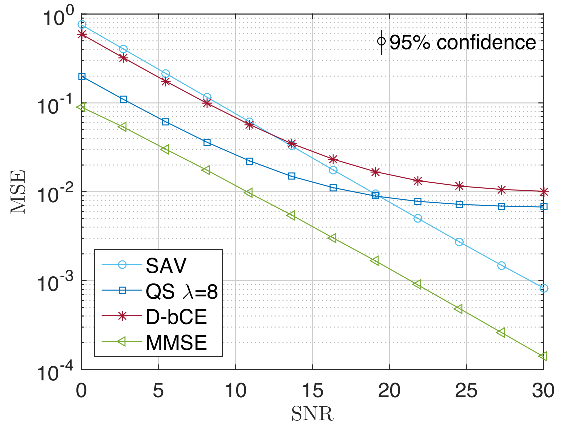

Fig. 4. MSE curves of proposed CE methods for a 2×2 transmission with $L = \gamma = 2$ on a TU channel.

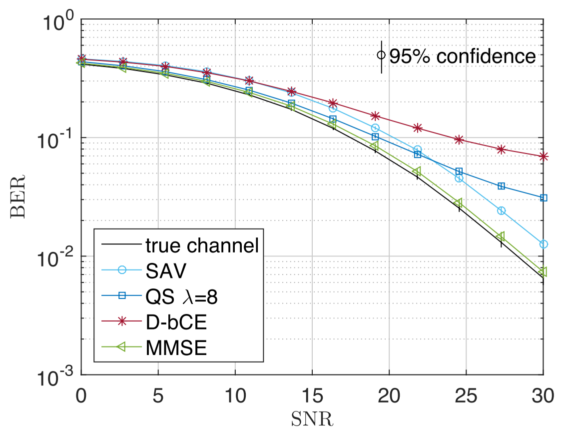

Fig. 5. BER curves for 16QAM with a zero forcing receiver.

MIMO transmission with $B = 72$ subarriers and a TU channel model [18]. The MSE curves of the proposed estimators are shown in Fig. 4. The corresponding uncoded bit error ratio (BER) curves are given in Fig. 5. As a reference, the DFT based CE (*D-bCE*) according to [3] and the MMSE estimator as given in (7) are shown.

The complexity of *D-bCE* is dominated by the FFT complexity of $\mathcal{O}(B\log(B))$. *MMSE* estimation complexity is dominated by a matrix inverse, i.e., $\mathcal{O}(B^3)$, ignoring the costs of estimating second order channel and noise statistics.

The sliding average CE method from Section V-A, denoted by *SAV*, shows a 1 dB penalty at low SNR in terms of MSE when compared to *D-bCE*. In the high SNR region it has the best MSE performance of the proposed schemes as is shows no error floor. Comparing the *SAV* MSE performance with *MMSE* estimation, *SAV* encounters a loss of 8 dB. This however, translates into a offset of approximately 2 dB in terms of BER. Considering that (11) only has linear complexity, i.e., $\mathcal{O}(B)$, this scheme is a low complexity alternative to *D-bCE*, that does not require any prior channel knowledge.

The quadratic smoothing estimation, denoted by *QS*, shows a significant MSE improvement at low SNR because it smooths over several observed channel coefficients. The high error floor shows that *QS* is not able to cancel all the inter-layer interference. *QS* performs uniformly better than *D-bCE* over the whole SNR range in terms of MSE and BER. For a fixed value of λ the matrix inverse in (15) can be precomputed, such that this method has a complexity of $\mathcal{O}(B^2)$ and does not exploit second order channel or noise statistics explicitly.

VII. Conclusion

We proposed low complexity channel estimation methods based on a matched filter (correlation) approach for frequency selective MIMO channels in the LTE-A uplink. Due to the DMRS allocation, the initial estimate contains severe inter-layer interference. This estimate is than significantly improved by exploiting either the DMRS structure in a sliding window post processing, or a smoothness prior in a smoothing scheme. Using a smoothness constraint on the channel leads to a significant performance improvement in the low SNR region. Since our methods completely operate in the frequency domain, they do not suffer from CIR leakage when a user is assigned a small bandwidth.

References

[1] X. Hou, Z. Zhang, and H. Kayama, “DMRS design and channel estimation for LTE-advanced MIMO uplink,” in *Proc. IEEE 70th VTC Fall*, Sep. 2009, pp. 1–5.
[2] H. Sahlin and A. Persson, “Aspects of MIMO channel estimation for LTE uplink,” in *Proc. IEEE VTC Fall*, Sep. 2011, pp. 1–5.
[3] Q. Zhang, X. Zhu, T. Yang, and J. Liu, “An enhanced DFT-based channel estimator for LTE-A uplink,” *IEEE Trans. Veh. Technol.*, vol. 62, no. 9, pp. 4690–4696, Nov. 2013.
[4] F. Liu, H. Wei, H. Zhao, and Y. Tang, “A novel channel estimation for MIMO SC-FDMA systems,” in *Proc. ICCCAS*, vol. 1, 2013, pp. 96–99.
[5] X. Zhang and Y. Li, “Optimizing the MIMO channel estimation for LTE-advanced uplink,” in *Proc. ICCVE*, Dec. 2012, pp. 71–76.
[6] X. Xia, H. Zhao, and C. Zhang, “Improved SRS design and channel estimation for LTE-Advanced uplink,” in *Proc. IEEE 5th Int. Symp. MAPE*, Oct. 2013, pp. 84–90.
[7] E. Dahlman, S. Parkvall, and J. Skold, *4G: LTE/LTE-Advanced for Mobile Broadband*. New York, NY, USA: IEEE, 2013.
[8] B. Sklar, “Rayleigh fading channels in mobile digital communication systems. i. characterization,” *IEEE Commun. Mag.*, vol. 35, no. 7, pp. 90–100, Jul. 1997.
[9] E. Zöchmann, S. Pratschner, S. Schwarz, and M. Rupp, “Limited feedback in OFDM systems for combating ISI/ICI caused by insufficient cyclic prefix length,” in *Proc. IEEE Asilomar Conf. Signals, Syst, Comput.*, Nov. 2014, pp. 988–992.
[10] E. Zöchmann, S. Pratschner, S. Schwarz, and M. Rupp, “MIMO transmission over high delay spread channels with reduced cyclic prefix length,” in *Proc. 19th Int. ITG WSA*, Mar. 2015, pp. 1–8.
[11] Technical specification group radio access networks; Physical Channels and Modulation (Release 12), 3rd Generation Partnership Project, Sophia Antipolis Cedex, France, Sep. 2014. [Online]. Available: http://www.3gpp.org/DynaReport/36211.htm
[12] C.-Y. Chen and D. Lin, “Channel estimation for LTE and LTE-A MU-MIMO uplink with a narrow transmission band,” in *Proc. ICASSP*, May 2014, pp. 6484–6488.
[13] S. M. Kay, *Fundamentals of Statistical Signal Processing: Estimation Theory*. Englewood Cliffs, NJ, USA: IEEE, 1993.
[14] S. Boyd and L. Vandenberghe, *Convex Optimization*. Cambridge, U.K.: IEEE, 2009.
[15] R. Gribonval, “Should penalized least squares regression be interpreted as maximum a posteriori estimation?” *IEEE Trans. Signal Process.*, vol. 59, no. 5, pp. 2405–2410, May 2011.
[16] S. Schwarz *et al.*, “Pushing the limits of LTE: A survey on research enhancing the standard,” *IEEE Access*, vol. 1, pp. 51–62, 2013.
[17] C. Mehlführer *et al.*, “The Vienna LTE simulators - enabling reproducibility in wireless communications research,” *EURASIP J. Adv. Signal Process.*, vol. 2011, no. 1, Dec. 2011.
[18] 3GPP TR25.943, Technical Specification Group Radio Access Networks; Deployment Aspects (Release 12), 3rd Generation Partnership Project, Sophia Antipolis Cedex, France, Oct. 2014. [Online]. Available: http://www.3gpp.org/ftp/Specs/html-info/25943.htm